A Miniaturized Cost Effective Shared Inductor based Energy Management System for Ultra-Low-Voltage Electromagnetic Energy Harvesters in Battery Powered Applications

Mahmoud Shousha[*†], Dragan Dinulovic[*], Michael Brooks[*], and Martin Haug[*]
Email: {mahmoud.shousha, dragan.dinulovic, michael.brooks, martin.haug}@we-online.de
[*]MagI[3]C R&D Division, Würth Elektronik eiSos GmbH & Co. KG, 85748 Garching bei München, Germany
[†]Electrical Power & Machines Dept., Faculty of Engineering, Cairo University, 12611, Giza, Egypt

***Abstract*— This paper presents a miniaturized and cost effective energy management system (EMS) for ultra-low-voltage electromagnetic energy harvesters (EMEHs) in battery powered applications. The EMS topology is based on utilizing a single inductor that is shared between positive and negative half cycles of the EMEH voltage and hence achieving system's cost and size reductions. Also, the EMS topology utilizes a smaller number of active components compared to existing solutions, used with ac harvesters, and hence allowing for further reduction in system's cost and simple implementation. The shared inductor is not only used by the power stage but also as a key part of the bias supply scheme. The EMS converts EMEH's ac voltage into a dc one in a single step and provides a maximum power point tracking (MPPT) feature to maximize the harvested energy.**

Experimental results show the effectiveness of the presented solution to provide MPPT for EMEH that has a damped voltage characteristics ranging from 1.2V to 10mV. The presented solution achieves 86.5% and 50% reductions in magnetics volume, which is the biggest contributor to the real estate of the EMS, compared to [1] and [2], respectively. Also, it can harvest more energy by 41.6% and 21.4% compared to [1] and [2], respectively, while reduces the BOM cost by 57.6% compared to [2].

Keywords— Electromagnetic energy harvesters; energy management system; shared-inductor topology, volume reduction, battery powered applications.

I. INTRODUCTION

Energy harvesting from ambient sources and body motion presents a potential solution to extend the operating time of batteries used in different applications. Extending battery operating time is of significant importance to reduce maintenance cost and/or human intervention within these systems. An example of these applications is integrating an energy harvester device in the shoes of athletes to harvest energy during running or jogging and storing the harvested energy in the battery used with wearable devices and smart watches to extend their operating time [3]-[5]. Another example, associated with medical applications, is legs transplant where a pressure sensor measures the pressure applied to the transplanted organ continuously and provides a warning or indication in case the user exceeds the rated specifications. This sensor is powered by a battery that needs to be active all the time when the users are moving. In case the battery is discharged while the user is still moving, there is a big risk that the transplanted organ is damaged. Harvesting energy when the transplanted organ hits the ground and storing this energy in the battery of the pressure sensor can be a solution for such a problem. The third application is extending the operating time of the batteries of electronic lock systems [6]-[7] for indoor applications. The integration of an energy harvesting device within the door such that it translates the door's movement into energy used to extend the operating time of the batteries that power the lock system. As a result, a significant reduction in maintenance cost associated with replacing the empty batteries can be achieved [7], especially in facilities which rely heavily on electronic door lock systems such as hotels and universities.

The targeted applications require an energy harvesting device that translate mechanical energy into electrical energy. The most commonly used energy harvesting devices that can achieve this criterion are electromagnetic energy harvesters

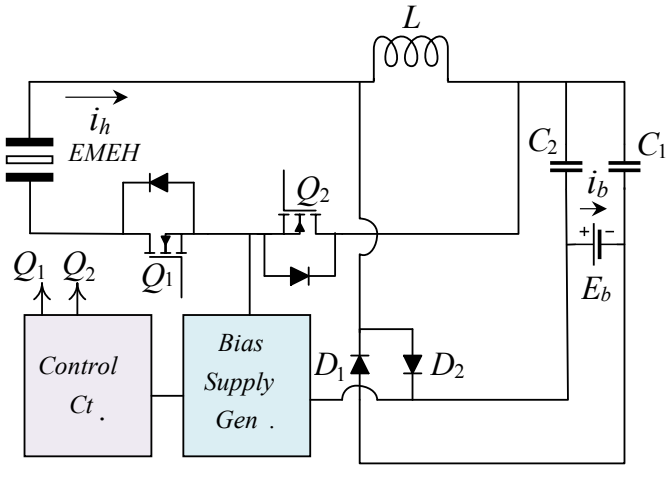

Fig.1: The presented EMS.

(EMEHs) [8]-[10] and piezoelectric generators [11]-[13]. Both types produce ac voltage and require maximum power point tracking (MPPT). Piezoelectric generators have the advantage of high output voltage [11], up to a few volts, which relaxes the requirements of the required EMS. On the other hand, it produces relatively low output power [11]-[13]. EMEHs have a higher output energy [9] while suffering from low output voltage, with ranges from few mVs to hundreds of mVs [8]-[10]. The availability of higher energy in EMEHs makes it more appealing for the targeted applications.

The main goal of this paper is to introduce the EMS, shown in Fig.1, which can operate with ultra-low-voltage EMEHs and provide an MPPT feature while achieving improvements in size, efficiency, and cost.

II. PRINCIPLE OF OPERATION

The EMS, shown in Fig.1 has the same principle of operation of resistance emulated converters used for power factor correction (PFC) applications [14]. The converter runs in discontinuous conduction mode (DCM) and hence it appears as a pure controlled resistive element to the EMEH. The input resistance of the EMS is matched with the output resistance of the EMEH and MPPT is achieved. It should be noted that the conventional solutions of using diode-based rectification [15]-[20] cannot be used with the EMEH due to the low output voltage levels of the harvester. As a result, the EMS topology needs to perform the ac-dc conversion in a single stage and without using diode(s) connected directly to the EMEH.

The EMS power stage consists of two mosfets, two diodes, a single inductor, and two output capacitors. L, Q_1, and Q_2, are active during positive and negative half cycles of the EMEH voltage while D_1 and C_1 are active during the positive half cycle, and D_2 and C_2 are active during the negative half cycle. Q_1 and Q_2 operate simultaneously and are used for energy transfer from the EMEH to L during the first part of the switching cycle, DTs, during both positive and negative half cycles. D_1 is used to transfer the stored energy in L to C_1 in the second part of the switching cycle, $(1\text{-}D)Ts$, during the positive half cycle while D_2 is used to transfer the stored energy in L to C_2 during the second part of the switching cycle in the negative half cycle. Figures 2.a-d show the modes of operation of the EMS power stage during positive and negative half cycles. The input impedance of the power stage of the EMS is similar to the input impedance of buck-boost converter and can be expressed as follows

$$Z_{in} = \frac{2f_s}{D^2}, \tag{1}$$

where Zin is the input impedance of the converter, L is the inductance value, fs is the switching frequency, and D is the duty cycle. In this work, the input impedance of the converter is controlled by adjusting the duty cycle and running at a constant switching frequency.

As it can be noted from Fig.2, the inductor is shared between the positive and negative half cycles, unlike the existing solutions that use two coupled inductors [1] or two inductors [2], hence size and cost improvements can be achieved. Another advantage of the arrangement of the topology is that Q1 and Q2 operate during the positive and negative half cycles and hence no synchronization with the input voltage is required which means a zero crossing detection circuit (ZCD) [2], [15], [17] is not needed which further helps in cost reduction of the introduced EMS.

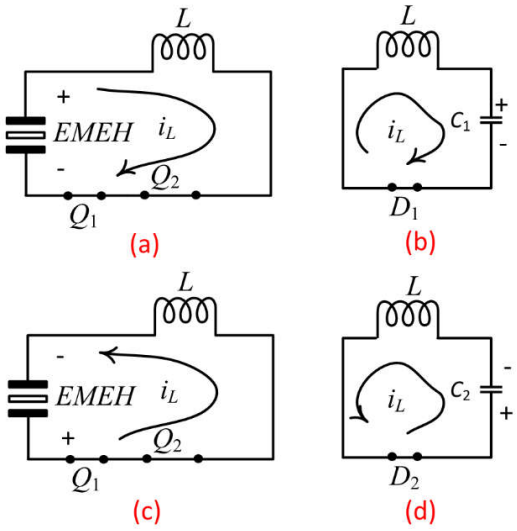

Fig.2: modes of operation of the EMS topology: (a) & (b) during the positive half cycle and (c) & (d) during the negative half cycle.

III. PRACTICAL IMPLEMENTATION

A. Bias Supply Scheme

The bias supply scheme used to power up the control circuit is based on a simple charge pump that utilizes the output capacitor, C_2, the EMEH voltage, and the power stage inductor to secure a sufficient bias supply voltage, v_{cc}, as shown in Figs 2.b and 3. Compared to the approaches presented in [2], [21], this bias supply scheme provides a higher output voltage while using fewer components than [2] and the same number of components as [21]. The bias voltage is expressed by the following equation (Figs. 3&2.b):

$$\begin{aligned} v_{cc} &= v_L + v_{c2} + v_{h,pk} - 2V_D \\ &= E_b + v_{h,pk} - 2V_D \end{aligned}, \tag{2}$$

where E_b is the battery voltage, vh,pk is the peak harvester voltage, and V_D is the threshold voltage of the diode. It should be noted that the ground of the bias scheme is the point of common sources of the two mosfetes such that the two mosfets can be easily driven directly from the control circuit. For a proper start-up, the bleeding resistor R_b, results in <1% losses, is connected across C_1 such that the battery voltage is

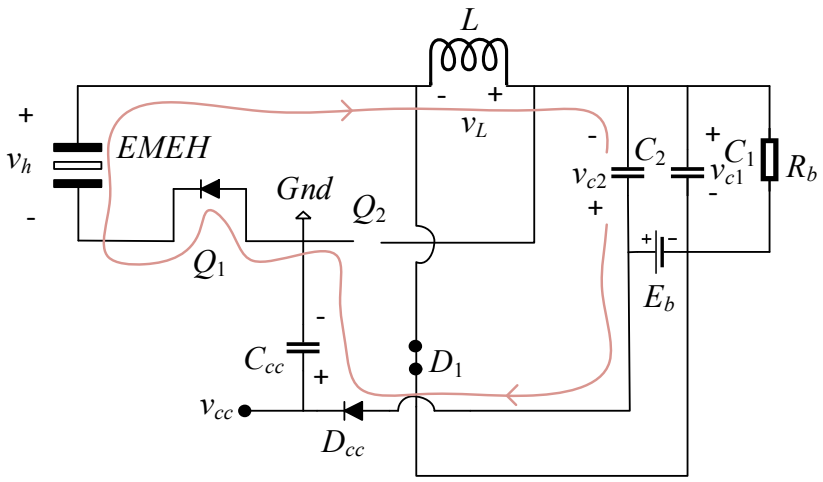

Fig.3: Operation of the bias supply scheme.

shared between C_1 and C_2 to avoid applying the full battery voltage across C_1 and hence failing of the bias scheme.

B. Control Circuit

The control circuit, shown in Fig.4, is based on two comparators [22] used to from an open loop pulse width modulator (PWM) [23]. The first comparator charges C_1 through R_3 and compares the voltage to v_x such that when the voltage across C_1 is higher than v_x the comparator resets and C_1 discharges to form a sawtooth signal as shown in Fig.4. The second comparator compares the sawtooth signal to v_y which determines the required input impedance of the power stage and produces PWM signals to Q_1 and Q_2. Different implementations of PWM exist [24]-[30] but this approach is chosen due to the ease of implementation with discrete components and low power consumption. The EMEH supplies its maximum available energy at loads which are equal to R_{opt}t±20% [9]-[10], which means it is not required to provide a tightly regulated bias supply voltage to provide perfect resistance matching. This relaxes the requirements of the control circuit by omitting the harvester's current and voltage sensing [2]. Figure 5 shows input impedance variations versus bias voltage variations from spice models simulations. It can be noted that less than 3% variation in the input impedance is achieved over the entire range of operation. That happens due to the fact that the control circuit operates in a weighted manner not an absolute one which means the ratio of the average value of the sawtooth signal to the set point remains the same while small variations in the switching frequency takes place due to variations in the ripples of the sawtooth signal.

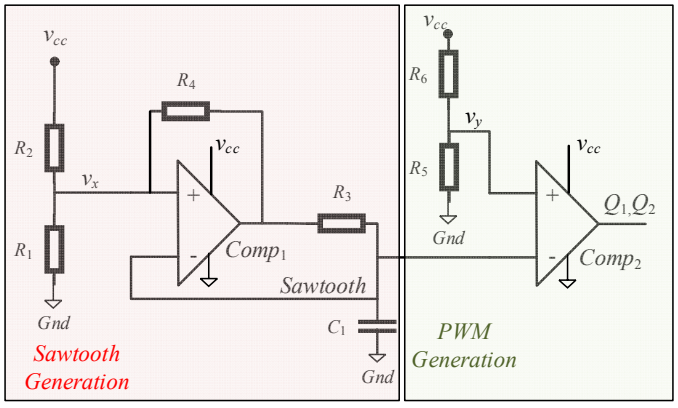

Fig.4: Control circuit schematic.

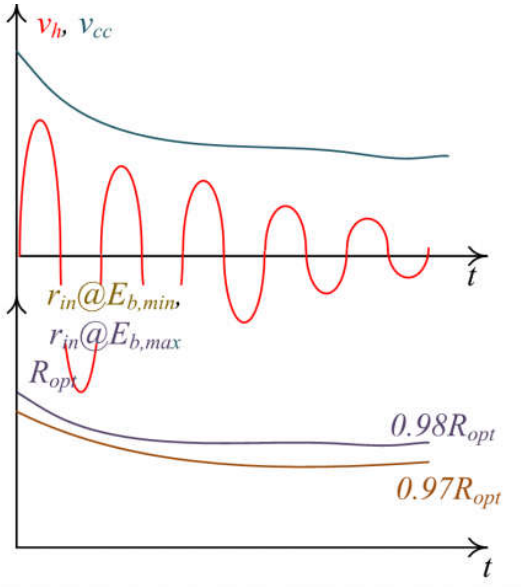

Fig.5: Input resistance variations.

IV. EXPERIMENTAL RESULTS

An experimental setup is built and tested to demonstrate the effectiveness of the presented approach. The optimal resistance of the EMEH is around 9.5 Ohms. Figure 6 shows MPPT capability of the EMS and it can be noted that the harvester current and voltage are in phase and have a similar shape with a ratio around 9.5. Figure 7 shows the harvested current. The EMS harvests around 17mJ, out of 20mJ, while the system presented in [1] harvests 12mJ [9] and the system in [2] harvests 14mJ [2]. The improvements in the harvested energy are due to achieving MPPT besides running the converter in DCM which reduces significantly the switching losses unlike [1] and using a lower components count than [1] and [2]. Figure 8 shows that input impedance variations versus cell voltage variations can be neglected, as explained in the previous section. Table 1 shows the bill of materials used to build the experimental setup. It should be noted that the experimental setup built in [2] uses additionally one more inductor, two more mosftes, pulse transformers for gate driving, and a zero crossing detection circuit which makes the presented system has a lower BOM cost by 57.6%. It is worth mentioning that the system presented in [1] is an integrated system and hence BOM comparison is not a straightforward task.

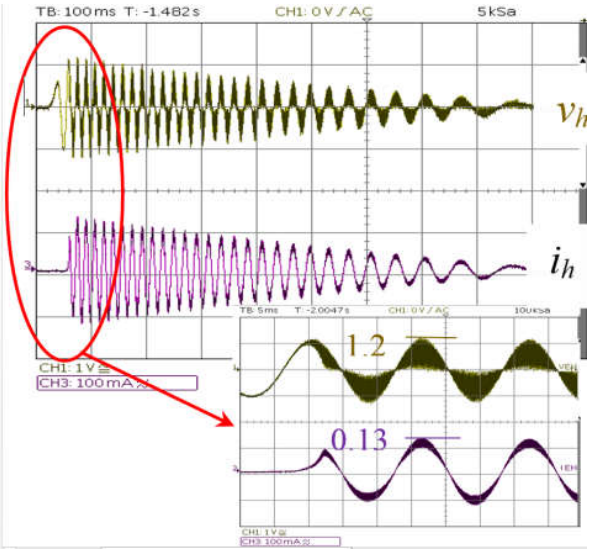

Fig. 6: Harvester's current and voltage.

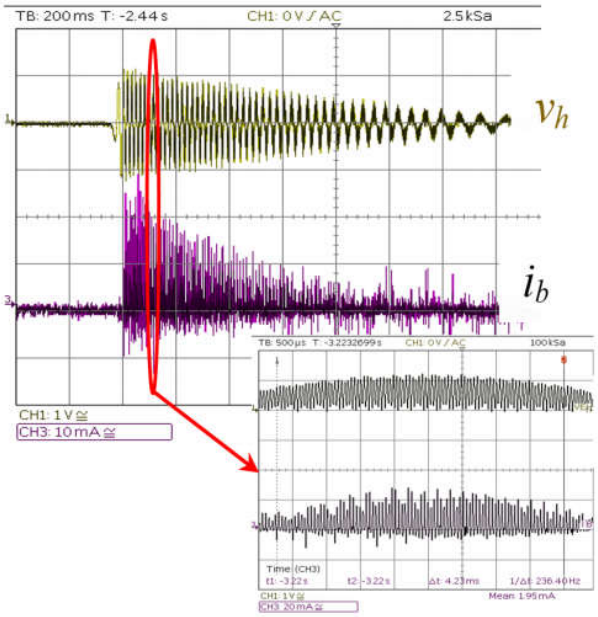

Fig.7: Harvester's voltage and the harvested current.

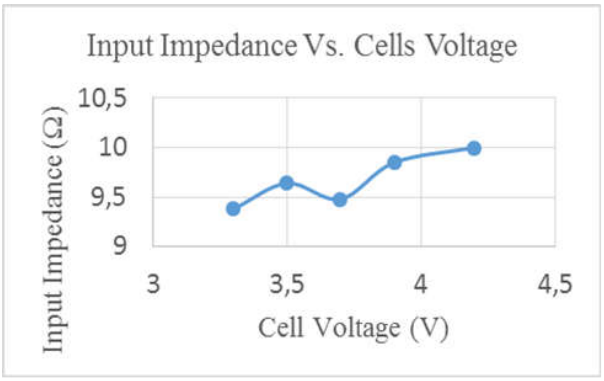

Fig. 8: Input impedance variation vs cell voltage.

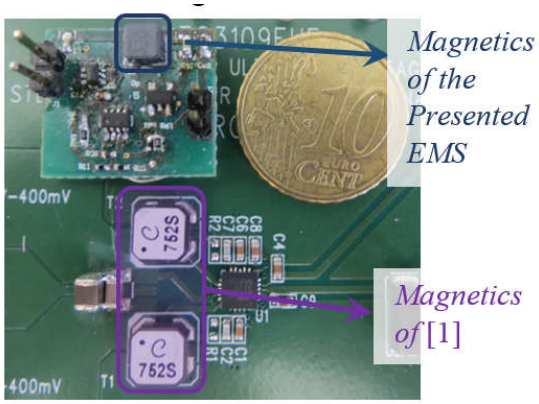

Fig.9: Experimental Setups comparison.

TABLE I. SYSTEM'S COMPONENTS

Item	*Description*
Mosfets	DMN3190LDW
Diodes for power stage	RB496EA
Diodes for bias supply scheme	PMEG2005ET
Comparators	TLV3691
Inductor	33µH, 0.4A
Ouput Capacitors	2X 10µF, 6.3V
Input Capacitor	0.1µF, 6.3V

V. CONCLUSIONS AND FUTURE WORK

This paper presented an EMS for ultra-low-voltage EMEH in battery powered applications. The EMS converts from ac to dc in a single step and provides an MPPT feature. Compared to the existing solutions, the EMS has a smaller size, higher efficiency, and lower cost. Future work includes IC implementation of the EMS and integration with passive components in a system-in-package (SiP) [31].

REFERENCES

[1] Linear Technology, "Auto-Polarity, Ultralow Voltage Step-Up Converter and Power Manager: LTC3109," datasheet, available: http://cds.linear.com/docs/en/datasheet/3109fb.pdf.

[2] M. Shousha, D. Dinulovic, and M. Haug, "A Universal Topology Based on Buck-Boost with Optimal Resistive Impedance Tracking for Energy Harvesters in Battery Powered Applications," in *Proc. 32nd Annu. IEEE Appl. Power Electron. Conf. Expo.,* pp.2111-2115, 2017.

[3] N.S. Shenck and J.A. Paradiso, "Energy Scavenging with Shoe-Mounted PiezoElectrics", *IEEE Micro*, vol. 21, no. 3, pp. 3041, May/June 2001.

[4] Jingjing Zhao and Zheng You, "A Shoe-Embedded Piezoelectric Energy Harvester for Wearable Sensors," *Sensors*, Vol. 14, no.7, pp. 12497–12510, July 2014.

[5] Gatto and E. Frontoni, "Energy Harvesting system for smart shoes," in *Proc. 10th IEEE/ASME Int. Conf. on Mechatronic and Embedded Syst. and Applicat.*, pp. 1-6, 2014.

[6] M. A. Webb, C. Christiansen, J. Hanchett, and S. Sullivan, "Electric door release powered by an energy harvester," European patent 2378041, Jan. 4, 2017.

[7] G. Cechmanek, "Small Scale Energy Harvesting for Use with an Electronic Door Strike," MASc thesis, University of Waterloo, Ontario, 2016.

[8] Q. Zhang, Y. Wang, and E. S. Kim, "Electromagnetic Energy Harvester With Flexible Coils and Magnetic Spring for 1–10 Hz Resonance", *Journal of Microelectromechanical Systems*, vol. 24, no. 4, pp. 1193 – 1206, Aug. 2015.

[9] D. Dinulovic, M. Shousha, M. Haug, and T. Petrovic, "Portable Rotational Electromagnetic Energy Harvester for IOT," in *Proc. IEEE Int. Mag. Conf.*, pp. 1-2, 2017.

[10] D. Dinulovic, M. Shousha, M. Brooks, M. Haug, and T. Petrovic, "Push-Button Rotational Electromagnetic Energy Harvesting System," in *Proc. 61st Annu. Conf. on Magnetism and Mag. Mater.*, pp.107, 2016.

[11] Z. Qin, H. Talleb, S. Yan, X. Xu and Z. Ren, "Application of PGD on Parametric Modeling of a Piezoelectric Energy Harvester," in *IEEE Trans. Mag.*, vol. 52, no. 11, pp. 1-11, Nov. 2016.

[12] A. Khaligh, P. Zeng and C. Zheng, "Kinetic Energy Harvesting Using Piezoelectric and Electromagnetic Technologies—State of the Art," in *IEEE Trans. Ind. Electron.*, vol. 57, no. 3, pp. 850-860, March 2010.

[13] F. Khameneifar, S. Arzanpour and M. Moallem, "A Piezoelectric Energy Harvester for Rotary Motion Applications: Design and Experiments," in *IEEE/ASME Trans. Mechatronics*, vol. 18, no. 5, pp. 1527-1534, Oct. 2013.

[14] R. W. Erickson and D. Maksimovic, "Fundamentals of Power Electronics," Springer Science & Business Media, 2007.

[15] R. J. Taylor, "Optimization of a Discontinuous Conduction Mode Flyback for Acoustical Energy Harvesting," M.S. thesis, University of Florida, Gainesville, Florida, 2004.

[16] L. Mateu, L. Lühmann, H. Zessin and P. Spies, "Modified parallel SSHI AC-DC converter for piezoelectric energy harvesting power supplies," in *Proc. 33rd Annu. IEEE Int. Telecomm. Energy Conf.*, pp. 1-7, 2011.

[17] M. Eltamaly and K. E. Addoweesh, "A Novel Self-Power SSHI Circuit for Piezoelectric Energy Harvester," in *IEEE Trans. Power Electron.*, vol. 32, no. 10, pp. 7663-7673, Oct. 2017.

[18] J. Dicken, P. D. Mitcheson, I. Stoianov, and E. M. Yeatman, "Power-Extraction Circuits for Piezoelectric Energy Harvesters in Miniature and Low-Power Applications," in *IEEE Trans. Power Electron.*, vol. 27, no. 11, pp. 4514-4529, Nov. 2012.

[19] M. Lallart, L. Garbuio, L. Petit, C. Richard, and D. Guyomar, "Double synchronized switch harvesting (DSSH): a new energy harvesting scheme for efficient energy extraction," in *IEEE Trans. Ultrason., Ferroelect., Freq. Control*, vol. 55, no.10, pp. 2119-2130, Oct. 2008.

[20] Y. Wu, A. Badel, F. Formosa, W. Liu, and A. Agbossou, "Self-powered optimized synchronous electric charge extraction circuit for piezoelectric energy harvesting," *J. Intell. Mater. Syst. and Structures*, vol. 25, no.15, pp. 2165-2176, Jan. 2014.

[21] M. Shousha, D. Dinulovic, and M. Haug, "Improved Bias Supply Scheme for a Maximum Power Point Tracking Universal Topology for Low-Voltage Electromagnetic Harvesters in Battery Powered Applications," in *Proc. Int. exhibition and Conf. for Power Electron., Intell. Motion, Renewable Energy, and Energy Manage.*, pp. 1-4, 2017.

[22] Texas Instrument, "TLV3691 0.9V to 6.5V, Nanopower Comparator," datasheet, 2015, available: http://www.ti.com/lit/ds/symlink/tlv3691.pdf.

[23] John D. Morris and Glen Brisebois, "Rail-to-Rail Output Dual Comparator Resolves 150MHz Signals While Shifting from Analog to Digital Voltage Levels," *Linear Technology Magazine*, March 2002.

[24] J. Wittmann and B. Wicht, "A configurable sawtooth based PWM generator with 2 ns on-time for >50 MHz DCDC converters," in *Proc. 11th Ph.D. Research in Microelectron. and Electron. Conf.*, pp. 41-44, 2015.

[25] J. Caldwell, "Analog Pulse Width Modulation," Texas Instrument Verified Reference Design, pp. 1-20, 2013, available: http://www.ti.com/lit/ug/slau508/slau508.pdf.

[26] B.J. Patella, A. Prodic, A. Zirger, D. Maksimovic, "High–Frequency Digital PWM Controller IC for DC–DC Converters," in *IEEE Trans. Power Electron.*, vol. 18, no. 1, pt. 2, pp. 438–446, January 2003.

[27] Z. Lukic, N. Rahman, and A. Prodic, "Multibit Σ–Δ PWM Digital Controller IC for DC– DC Converters Operating at Switching Frequencies Beyond 10 MHz," in *IEEE Trans. Power Electron.*, Vol. 22 , no 5, 2007 pp. 1693 – 1707.

[28] A. Prodic and D. Maksimovic, "Digital PWM controller and current estimator for a low power switching converter" in *Proc. 7th IEEE Workshop on Computers in Power Electron.*, pp.123-128, 2000.

[29] M. G. Batarseh, W. Al-Hoor, L. Huang, C. Iannello and I. Batarseh, "Window-Masked Segmented Digital Clock Manager-FPGA-Based Digital Pulse width Modulator Technique," in *IEEE Trans. Power Electron.*, vol. 24, no. 11, pp. 2649-2660, Nov. 2009.

[30] O. Trescases, Guowen Wei, and Wai Tung Ng, "A Segmented Digital Pulse Width Modulator with Self-Calibration for Low-Power SMPS," in *Proc. IEEE Conf. on Electron. Devices and Solid-State Circuits*, pp.367-370, 2005.

[31] S. Wolf, J. Stephan, and R. Regenhold, "ABC of Power Modules: Functionality, Structure and Hanlding of a Power Module," Swiridoff Verlag, 2015.